JOURNAL OF MOLECULAR SPECTROSCOPY **192,** 348–358 (1998)
ARTICLE NO. MS987700

Fourier Transform Emission Spectroscopy of the $A^2\Pi$–$X^2\Sigma^+$ Transition of BeD

C. Focsa,[1] P. F. Bernath,[2] R. Mitzner, and R. Colin

Laboratoire de Chimie Physique Moléculaire, Université Libre de Bruxelles, C.P. 160/09, 50 av. F. D. Roosevelt, 1050-Brussels, Belgium

Received June 19, 1998

The $A^2\Pi$–$X^2\Sigma^+$ $\Delta v = 0$ sequence of BeD was observed in the 19 500–20 800 cm^{-1} spectral region using a Fourier transform spectrometer. The emission spectrum was excited in a Be hollow cathode discharge lamp with a He/D_2 gas mixture. The observed lines were assigned to the 0–0 to 6–6 bands. The $\Delta v = -1$ sequence was too weak to be seen in our Fourier transform spectra. We therefore used a previously recorded but unpublished arc emission spectrum to identify the 0–1 to 5–6 $\Delta v = -1$ bands. Consequently, all of the diagonal bands could be linked together and the vibrational intervals determined. The $\Delta v = 0$ and $\Delta v = -1$ data were fitted together in a global fit and effective constants derived. Using the information available from the study of the $C^2\Sigma^+$–$X^2\Sigma^+$ system [R. Colin, C. Drèze, and M. Steinhauer, *Can. J. Phys.* **61,** 641 (1983)], the $v = 8$–12 vibrational levels of the ground state were added in a Dunham fit. A set of Dunham *Y* constants was determined for the $X^2\Sigma^+$ state along with traditional equilibrium parameters for the $A^2\Pi$ excited state. The equilibrium bond lengths were found to be 1.341742(5) Å for the ground state and 1.33309(4) Å for the excited state. A reanalysis of the previously published $A^2\Pi$–$X^2\Sigma^+$ 0–0 to 3–3 $\Delta v = 0$ bands of BeT [D. De Greef and R. Colin, *J. Mol. Spectrosc.* **53,** 455–465 (1974)] was also performed.

I. INTRODUCTION

We have recently reanalyzed the $A^2\Pi$–$X^2\Sigma^+$ spectrum of BeH (*1*) and were able to link all of the bound ground state vibrational levels from $v'' = 0$–10. At the same time, we recorded new Fourier transform emission spectra of BeD using the same hollow cathode source. Since BeH, BeD, and BeT are relatively light molecules, they can be used to study the breakdown of the Born–Oppenheimer approximation and to benchmark open-shell *ab initio* calculations (*1–3*).

In our recent BeH paper (*1*) we have reviewed the literature for BeH, BeD, and BeT, so we will make only a few specific comments about BeD and BeT. The first BeD spectra were recorded by Koontz (*4*) using an arc source. Only the $A^2\Pi$–$X^2\Sigma^+$ transition was studied and these measurements were improved and extended to other systems by Colin and coworkers using a King furnace (*5–7*). For the $A^2\Pi$–$X^2\Sigma^+$ transition, data are available for BeD for only the 0–0, 1–1, and 2–2 bands (*4–5*), while the 0–0, 1–1, 2–2, and 3–3 bands are known (*2*) for BeT. The $A^2\Pi$–$X^2\Sigma^+$ system of BeT was recorded, for safety reasons, with a hollow cathode source (*2*). Very recently the $A^2\Pi$–$X^2\Sigma^+$ system of BeD was identified in emission from a tokamak plasma (*8*).

For BeD, we recorded the 0–0 to 6–6 vibrational bands of the $A^2\Pi$–$X^2\Sigma^+$ system and linked them together using the 0–1 to 5–6 bands recorded with an arc source. The off-diagonal bands of the *A*–*X* system are very weak, with Franck–Condon factors of about 0.002, and could not be studied by Fourier transform emission spectroscopy (*1*). We, therefore, had to use unpublished data from an arc source recorded with a 2-m spectrograph (*9*).

There is additional information available for the ground state for $v'' = 8$–12 from the $C^2\Sigma^+$–$X^2\Sigma^+$ transition (*9*). The weak $C^2\Sigma^+$–$X^2\Sigma^+$ transition can only be seen in emission with a bright arc source. Unfortunately, we could not directly bridge the gap between $v'' = 6$ and 8, but we did include ground state rotational and vibrational combination differences for the $v'' = 8$–12 levels of BeD in a fit using Dunham *Y*'s (*10*). For BeH we were more fortunate and could link all of the bound ground state vibrational levels together (*1*). The old BeT data (*2*) have also been recalibrated and refitted using the same Hamiltonian matrices as used for BeH and BeD.

In this paper we report new line positions and spectroscopic constants for BeD and BeT that we intend to use in the future for an $A^2\Pi$–$C^2\Sigma^+$ deperturbation analysis and for a more detailed study of the breakdown of the Born–Oppenheimer approximation.

II. EXPERIMENTAL DETAILS

Two kinds of spectra have been used for the analysis of the $A^2\Pi$–$X^2\Sigma^+$ system of BeD. The $\Delta v = 0$ sequence was excited in a Be hollow cathode discharge and recorded using a Fourier transform spectrometer. Attempts to excite the $\Delta v = -1$

[1] Permanent address: Laboratoire de Physique des Lasers, Atomes et Molécules, UMR CNRS, Centre d'Etudes et de Recherches Lasers et Applications, Université des Sciences et Technologies de Lille, 59 655 Villeneuve d'Ascq Cedex, France.

[2] Permanent address: Department of Chemistry, University of Waterloo, Waterloo, Ontario, Canada N2L 3G1.

0022-2852/98 $25.00

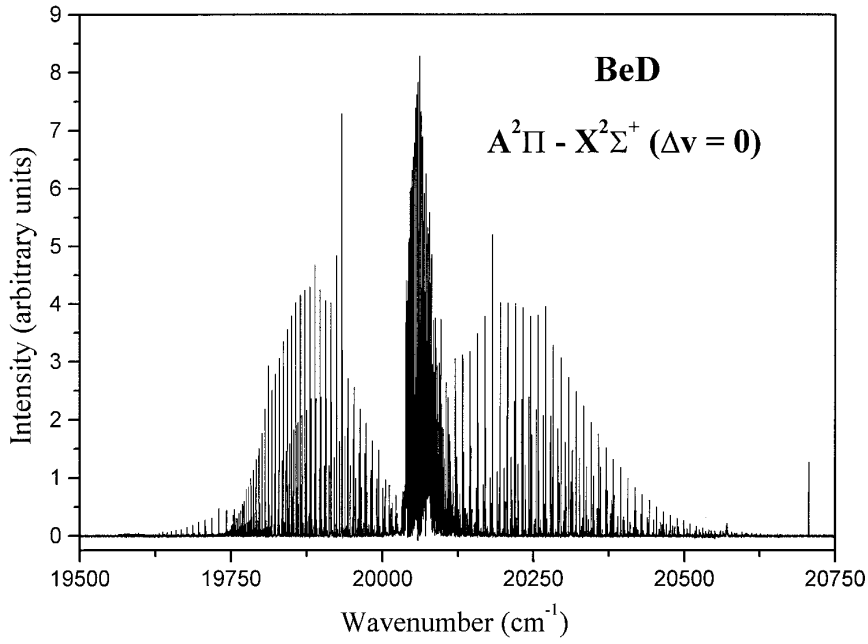

FIG. 1. An overview of the $A^2\Pi$–$X^2\Sigma^+$ ($\Delta v = 0$) FT emission spectrum of BeD. Some weak impurity lines belonging to the $A^2\Pi$–$X^2\Sigma^+$ 0–0 band of BeH can be observed to lower wavenumbers at 19 750 cm^{-1}.

sequence in the hollow cathode source were unsuccessful. Consequently, we have used a previously recorded, but unpublished, arc emission spectrum (*9*) of the $\Delta v = -1$ sequence to link the new FTS bands together. A separate description of the two experimental procedures is given below.

The Be hollow cathode used to excite the $A^2\Pi$–$X^2\Sigma^+$ ($\Delta v = 0$) sequence was operated at currents of ~700 mA with a nonflowing mixture of He (80%) and D_2 (20%) at a pressure of 8 Torr. The optimal experimental conditions were obtained when the discharge had an intense blue color. The emission from the discharge

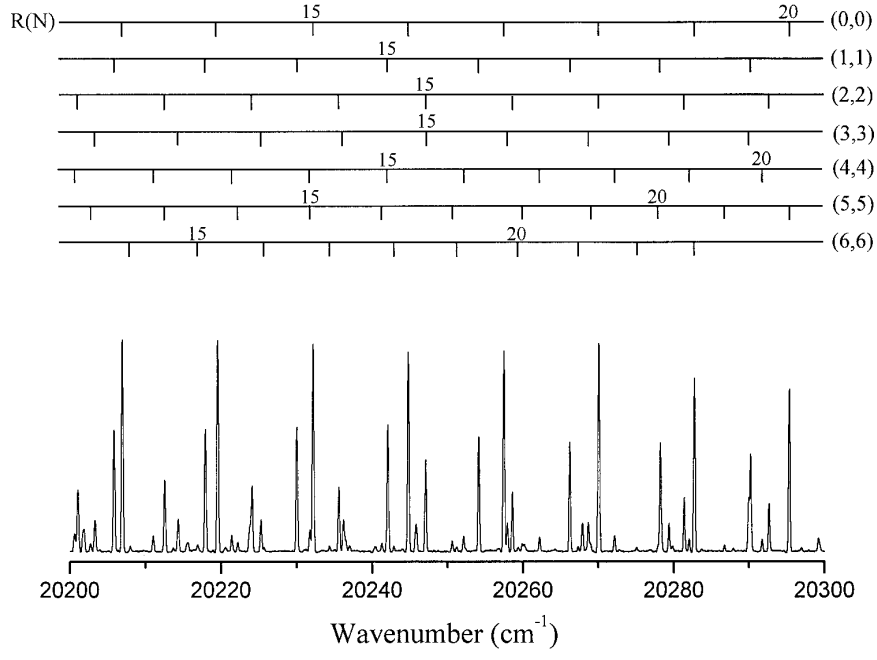

FIG. 2. An expanded portion of the $A^2\Pi$–$X^2\Sigma^+$ $\Delta v = 0$ sequence of BeD displaying several *R* lines of the 0–0 to 6–6 bands. The unmarked lines belong to BeH.

TABLE 1
Observed Line Positions (in cm^{-1}) for the $A^2\Pi$–$X^2\Sigma^+$ $\Delta v = 0$ and $\Delta v = -1$ Sequences of BeD

		$A^2\Pi - X^2\Sigma^+$					
		0 – 0			1 – 1		
N		R(N)	P(N)	Q(N)	R(N)	P(N)	Q(N)
0	*e*	20049.582(3)			20065.760(27)		
1	*e*	20060.906(-31)		20038.306(-15)	20076.817(16)		20054.699(-28)
	f	20060.131(3)		20036.750(-4)	20075.934(-46)		20053.187(49)
2	*e*	20072.504(-8)	20015.841(0)	20038.395(-27)	20088.032(-37)	20032.755(3)	20054.777(-14)
	f	20071.969(2)	20014.302(28)	20037.615(1)	20087.533(17)	20031.243(74)	20053.950(-21)
3	*e*	20084.188(-58)	20004.738(6)	20038.801(53)	20099.493(13)	20021.836(-20)	20055.069(6)
	f	20083.842(2)	20003.937(13)	20038.250(49)	20099.065(-1)	20021.044(5)	20054.544(35)
4	*e*	20096.118(7)	19993.886(6)	20039.260(16)	20111.032(29)	20011.198(-4)	20055.498(9)
	f	20095.758(-36)	19993.317(-15)	20038.801(-36)	20110.658(-22)	20010.648(0)	20055.069(-6)
5	*e*	20108.125(32)	19983.244(8)	20039.914(21)	20122.651(25)	20000.743(5)	20056.064(14)
	f	20107.815(-24)	19982.809(-19)	20039.563(-13)	20122.346(-20)	20000.322(-2)	20055.703(-25)
6	*e*	20120.183(3)	19972.800(9)	20040.716(27)	20134.342(7)	19990.461(7)	20056.752(12)
	f	20119.944(-29)	19972.464(-9)	20040.413(-22)	20134.109(-14)	19990.126(-6)	20056.466(-15)
7	*e*	20132.374(13)	19962.554(11)	20041.648(23)	20146.132(12)	19980.363(11)	20057.564(11)
	f	20132.142(-50)	19962.277(-12)	20041.398(-22)	20145.931(-15)	19980.082(-10)	20057.323(-18)
8	*e*	20144.574(-53)	19952.505(8)	20042.705(4)	20157.924(-48)	19970.435(5)	20058.484(0)
	f		19952.270(-21)	20042.487(-45)		19970.200(-18)	20058.338(25)
9	*e*	20156.927(-43)	19942.654(-1)	20043.936(24)	20169.835(-47)	19960.689(-5)	20059.546(9)
	f		19942.452(-36)	20043.736(-38)		19960.487(-34)	20059.363(-31)
10	*e*	20169.341(-39)	19932.974(-51)	20045.195(-63)	20181.816(-25)	19951.191(40)	20060.674(-28)
	f					19951.015(5)	
11		20181.816(-33)	19923.526(-84)	20046.695(-43)	20193.804(-36)	19941.747(-56)	20061.938(-46)
12		20194.354(-16)	19914.364(-51)	20048.312(-37)	20205.844(-26)	19932.606(-49)	20063.354(-24)
13		20206.917(-14)	19905.410(-35)	20050.064(-27)	20217.900(-23)	19923.634(-78)	20064.878(-4)
14		20219.516(-10)	19896.678(-27)	20051.944(-17)	20229.969(-18)	19914.948(-31)	20066.460(-35)
15		20232.139(-7)	19888.178(-22)	20053.950(-8)	20242.033(-24)	19906.434(-25)	20068.183(-31)
16		20244.778(-3)	19879.916(-16)	20056.064(-15)	20254.112(-9)	19898.138(-18)	20070.017(-19)
17		20257.424(-1)	19871.897(-11)	20058.338(14)	20266.167(-5)	19890.061(-13)	20071.951(-8)
18		20270.050(-16)	19864.123(-7)	20060.674(-12)	20278.207(6)	19882.209(-7)	20073.972(-9)
19		20282.702(2)	19856.598(-3)	20063.184(14)	20290.197(0)	19874.579(-6)	20076.118(18)
20		20295.320(5)	19849.325(0)	20065.766(0)	20302.155(3)	19867.181(-1)	20078.284(-24)
21		20307.907(6)	19842.306(2)	20068.492(15)	20314.061(4)	19860.012(0)	20080.655(46)
22		20320.460(7)	19835.543(4)	20071.320(22)	20325.909(7)	19853.073(0)	20082.997(3)
23		20332.969(8)	19829.040(7)	20074.232(8)	20337.688(9)	19846.372(4)	20085.468(6)
24		20345.425(8)	19822.795(7)	20077.264(11)	20349.387(10)	19839.911(13)	20088.038(31)
25		20357.821(10)	19816.811(8)	20080.388(4)	20361.018(29)	19833.670(8)	20090.637(11)
26		20370.143(9)	19811.084(3)	20083.621(11)	20372.514(11)	19827.670(7)	20093.321(5)
27		20382.387(9)	19805.617(-2)	20086.963(36)	20383.923(13)	19821.916(20)	20096.118(49)
28		20394.542(8)	19800.437(17)	20090.337(5)	20395.202(1)	19816.369(6)	20098.965(82)
29		20406.596(3)	19795.488(8)	20093.791(-28)	20406.366(2)	19811.084(22)	20101.755(4)
30		20418.551(7)	19790.806(6)	20097.399(13)	20417.400(10)	19806.003(14)	20104.711(44)
31		20430.382(2)	19786.382(5)	20101.034(9)	20428.274(4)	19801.153(9)	20107.617(-8)
32		20442.092(1)	19782.212(4)	20104.711(-20)	20438.992(1)	19796.522(1)	20110.658(38)
33		20453.669(3)	19778.302(11)	20108.511(11)	20449.549(6)	19792.119(0)	20113.662(18)
34		20465.097(0)	19774.624(1)	20112.338(16)	20459.915(1)	19787.938(5)	20116.724(34)
35		20476.368(-2)	19771.196(-2)	20116.190(-2)	20470.088(-5)	19783.956(0)	20119.784(34)
36		20487.476(-4)	19768.019(4)	20120.133(28)	20480.051(-18)	19780.183(-3)	20122.841(24)
37		20498.385(-27)	19765.055(-9)	20124.049(-1)	20489.825(-4)	19776.609(-6)	20125.937(56)
38		20509.153(-4)	19762.334(-9)	20128.019(-3)	20499.340(-20)	19773.236(-1)	20128.932(0)
39		20519.722(19)	19759.841(-4)	20132.025(13)	20508.611(-37)	19770.034(-10)	20132.032(68)
40		20530.075(37)	19757.550(-13)	20135.984(-24)	20517.686(4)	19767.080(50)	20134.937(-26)
41		20540.183(35)	19755.499(10)	20139.997(-8)	20526.442(-1)	19764.199(16)	20137.893(-27)
42		20550.088(65)	19753.587(-27)	20143.971(-18)	20534.973(53)	19761.476(-19)	20140.804(-19)
43		20559.671(25)	19751.902(-29)	20147.963(11)	20543.154(59)	19758.934(-24)	20143.608(-52)
44		20568.945(-60)	19750.433(2)	20151.847(-34)	20551.017(66)	19756.565(4)	20146.483(64)
45		20578.065(-21)	19749.095(-4)	20155.743(-22)	20558.447(-23)	19754.277(-13)	20149.108(25)
46		20586.882(9)	19747.964(32)	20159.610(19)	20565.537(-99)	19752.160(23)	20151.607(-32)

Note. "Observed − calculated" differences are reported in parentheses, in units of the last quoted digit (see text).

was recorded with a Bruker IFS 120 HR Fourier transform spectrometer. An Si photodiode detector and a band-pass filter were used to isolate the 18 000–22 500 cm^{-1} spectral region. A total of 25 scans were coadded in about 15 min of observation at an instrumental resolution of 0.1 cm^{-1}. Higher resolution spectra were not recorded because the uncooled cathode (necessary to vaporize Be) had a temperature of about 1500 K. The resulting Doppler widths of the BeD lines were about 0.2 cm^{-1}. The wavelength scale was calibrated against BeH molecular lines present in the spectrum as an impurity. The BeH spectrum (*1*) had been previously calibrated using Ne atomic lines (*11*). The estimated absolute accuracy of the wavenumber scale is ±0.003

TABLE 1—*Continued*

	0 – 0			1 – 1		
N	R(N)	P(N)	Q(N)	R(N)	P(N)	Q(N)
47	20595.394(45)	19746.919(6)	20163.330(-14)	20572.397(-31)	19750.056(-30)	20154.072(-2)
48	20603.481(-15)	19746.053(23)	20167.043(30)	20578.724(-101)	19748.181(56)	20156.356(-14)
49	20611.331(33)	19745.306(33)	20170.615(35)	20584.789(-18)	19746.248(10)	20158.571(61)
50	20618.776(41)	19744.601(-25)	20174.091(60)	20590.355(5)		20160.510(36)
51			20177.376(29)	20595.509(80)		
52			20180.554(42)	20600.050(33)		
53			20183.584(78)	20604.142(53)		
54			20186.374(63)			
55			20188.986(82)			
56			20191.421(157)			

		2 – 2			3 – 3		
N		R(N)	P(N)	Q(N)	R(N)	P(N)	Q(N)
1	*e*				20094.544(-30)		
	f				20093.791(74)		20071.951(18)
2	*e*				20105.190(-13)		
	f				20104.711(83)		
3	*e*	20110.082(-16)	20034.436(34)		20115.944(11)		
	f	20109.680(-4)	20033.595(22)		20115.487(-20)		20073.076(-82)
4	*e*	20121.275(8)	20023.934(-4)	20067.196(66)	20126.759(23)	20031.893(-22)	
	f	20120.939(-7)	20023.397(16)	20066.766(49)	20126.385(-22)	20031.334(-5)	
5	*e*	20132.494(-20)	20013.642(-5)	20067.607(15)	20137.600(3)	20021.836(42)	
	f	20132.242(-17)	20013.232(-2)	20067.196(-75)	20137.353(15)	20021.360(-8)	
6	*e*	20143.871(42)	20003.525(7)	20068.183(20)	20148.513(10)	20011.800(-11)	
	f	20143.608(-16)	20003.190(-7)	20067.879(-28)	20148.260(-36)	20011.487(2)	
7	*e*	20155.213(13)	19993.558(10)	20068.863(26)	20159.510(66)	20001.983(14)	20075.337(21)
	f	20155.005(-28)	19993.317(23)	20068.592(-39)	20159.292(13)	20001.704(-5)	
8	*e*	20166.603(-14)	19983.753(14)	20069.616(5)	20170.478(68)	19992.272(6)	20075.939(20)
	f	20166.430(-54)	19983.521(-13)	20069.424(-22)	20170.374(96)	19992.035(-23)	20075.769(14)
9	*e*	20178.029(-43)	19974.090(-6)	20070.463(-20)	20181.317(-73)	19982.809(102)	20076.650(50)
	f		19973.892(-38)	20070.315(-35)		19982.535(-6)	20076.480(11)
10	*e*	20189.537(-19)	19964.631(7)	20071.420(-32)	20192.337(-41)	19973.312(16)	20077.264(-88)
	f		19964.454(-36)			19973.139(-24)	
11		20201.037(-23)	19955.283(-42)	20072.504(-10)	20203.329(-33)	19963.990(-47)	20078.184(5)
12		20212.548(-24)	19946.112(-95)	20073.623(-45)	20214.310(-23)	19954.894(-42)	20079.091(17)
13		20224.073(-13)	19937.235(-36)	20074.883(-28)	20225.264(-16)	19946.012(17)	20080.028(-7)
14		20235.586(-5)	19928.536(11)	20076.218(-23)	20236.196(-1)	19937.235(17)	20081.007(-53)
15		20247.076(-3)	19919.954(-14)	20077.660(4)	20247.076(4)	19928.536(-72)	20082.141(-4)
16		20258.541(2)	19911.600(-6)	20079.091(-60)	20257.891(-3)	19920.174(4)	20083.247(-43)
17		20270.050(87)	19903.444(1)	20080.655(-71)	20268.655(0)	19911.906(0)	20084.516(27)
18		20281.349(8)	19895.481(3)	20082.374(-1)	20279.346(1)	19903.815(0)	20085.836(98)
19		20292.673(10)	19887.720(2)	20084.188(89)	20289.930(-22)	19895.910(5)	20086.963(-71)
20		20303.921(2)	19880.169(8)	20085.836(-53)	20300.477(9)	19888.178(6)	20088.405(30)
21		20315.109(9)	19872.816(5)	20087.735(-10)	20310.868(-14)	19880.625(7)	20089.696(-56)
22		20326.200(4)	19865.677(8)	20089.696(34)	20321.189(6)	19873.257(10)	20091.157(-8)
23		20337.202(5)	19858.742(8)	20091.650(15)	20331.369(9)	19866.043(-11)	20092.638(31)
24		20348.097(6)	19852.019(12)	20093.671(11)	20341.401(0)	19859.043(-1)	20094.145(71)
25		20358.876(5)	19845.518(29)	20095.758(27)	20351.298(2)	19852.223(9)	20095.608(50)
26		20369.525(2)	19839.155(-21)	20097.836(-7)	20361.018(-15)	19845.518(-42)	20097.042(-11)
27		20380.023(-14)	19833.078(8)	20100.020(28)	20370.599(-3)	19839.155(70)	20098.523(-34)
28		20390.408(3)	19827.166(-1)	20102.176(5)	20380.023(32)	19832.767(-15)	20100.020(-40)
29		20400.606(-6)	19821.457(-8)	20104.399(25)	20389.187(2)	19826.697(43)	20101.605(47)
30		20410.639(-9)	19815.960(-3)	20106.581(-12)	20398.173(0)	19820.686(-5)	20103.052(13)
31		20420.539(36)	19810.648(-8)	20108.795(-28)	20406.947(4)	19814.891(-5)	20104.499(0)
32		20430.141(-20)	19805.617(77)	20111.032(-23)	20415.460(-19)	19809.261(0)	20105.948(18)
33		20439.589(-24)	19800.537(-72)	20113.304(21)	20423.767(-5)	19803.782(0)	20107.320(-2)
34		20448.848(1)	19795.878(16)	20115.487(-9)	20431.794(-11)	19798.449(-7)	20108.651(-18)
35		20457.840(-5)	19791.275(-13)	20117.643(-45)	20439.589(24)	19793.270(-6)	20109.987(27)
36		20466.584(-14)	19786.870(-15)	20119.844(-4)	20447.038(2)	19788.186(-53)	

cm^{-1}. The line positions were measured by fitting Voigt lineshape functions to the experimental lines in a nonlinear, least-squares procedure. The precision of our measurements is estimated to about ± 0.01 cm^{-1} for unblended lines. The doublet fine-structure splitting of the molecular lines could be measured at low N values (up to $N \sim 10$).

The experimental setup used to record the $A^2\Pi$–$X^2\Sigma^+$ ($\Delta v = -1$) sequence was previously described in detail by Colin *et al.* (*9*) in their study of the $C^2\Sigma^+$–$X^2\Sigma^+$ system and only a brief description will be given here. A conventional arc source with Be electrodes was used to excite the spectrum. The arc was operated at 190 V, 9 A dc current, with a 1:5 mixture of H_2 and Ar at a total pressure of a few Torr. The emission spectra were photographed in the second order of a 2-m Czerny–Turner grating spectrograph, using Kodak I–F plates and 50-μm slits. The emission spectrum of an iron hollow cathode was used for wavelength calibration. The absolute error in the line positions is estimated to be 0.2 cm^{-1} and the uncertainty in the relative line positions is better than 0.1 cm^{-1} for strong unblended lines.

TABLE 1—*Continued*

	2 – 2			3 – 3		
N	R(N)	P(N)	Q(N)	R(N)	P(N)	Q(N)
37	20475.084(-7)	19782.656(10)	20121.962(-5)	20454.203(2)	19783.305(-30)	
38	20483.314(5)	19778.503(-57)	20124.049(14)	20461.057(9)		
39	20491.230(-7)	19774.624(1)	20126.037(-3)	20467.584(25)		
40	20498.874(14)	19770.782(-40)	20128.019(47)	20473.793(77)		
41	20506.190(30)	19767.080(-73)	20129.853(34)	20479.547(45)		
42	20513.151(31)	19763.618(15)	20131.525(-42)			
43		19760.256(95)				

		4 – 4			5 – 5		
N		R(N)	P(N)	Q(N)	R(N)	P(N)	Q(N)
5	*e*		20025.072(6)				
	f		20024.626(-28)				
6	*e*	20148.260(30)	20015.256(21)		20143.066(-3)	20004.315(3)	
	f	20147.963(-70)	20014.912(-7)		20142.844(-19)	20003.937(-110)	
7	*e*	20158.730(2)	20005.549(29)		20153.095(-8)	19994.830(16)	
	f	20158.571(-1)	20005.271(-1)		20152.955(11)	19994.574(-33)	
8	*e*	20169.181(-45)	19995.939(18)	20077.264(-47)	20163.150(34)	19985.404(-10)	
	f		19995.704(-21)	20077.264(107)	20162.974(-19)	19985.207(-47)	
9	*e*	20179.698(-20)	19986.461(16)	20077.812(20)	20173.098(1)	19976.056(-60)	
	f		19986.258(-31)	20077.660(-9)			
10		20190.134(-56)	19977.042(-49)	20078.284(-37)	20183.046(11)	19966.901(-23)	
11		20200.599(-36)	19967.830(-39)		20192.909(-13)	19957.827(-16)	
12		20211.015(-27)	19958.741(-37)	20079.506(-18)	20202.734(-13)	19948.864(-11)	
13		20221.386(-15)	19949.798(-26)		20212.548(46)	19940.013(-11)	
14		20231.708(4)	19940.992(-18)		20222.179(4)	19931.276(-17)	
15		20242.033(95)	19932.270(-69)	20081.614(-24)	20231.708(-45)	19922.691(6)	
16		20252.099(6)	19923.804(-11)	20082.374(-41)	20241.245(14)	19914.205(5)	
17		20262.157(-3)	19915.438(0)	20083.247(26)	20250.598(4)	19905.861(18)	
18		20272.125(-5)	19907.210(-1)	20084.022(-29)	20259.840(8)	19897.606(-5)	
19		20282.005(13)	19899.146(8)	20084.931(26)	20268.955(21)	19889.512(1)	
20		20291.751(19)	19891.211(-5)		20277.851(-36)	19881.534(-3)	
21		20301.361(18)	19883.486(37)	20086.643(-15)	20286.681(0)	19873.712(17)	
22		20310.868(56)	19875.842(6)	20087.519(-30)	20295.320(15)	19866.043(64)	
23		20320.022(-105)	19868.392(15)	20088.405(-39)	20303.734(-7)	19858.353(-39)	
24		20329.304(24)	19861.074(2)	20089.339(2)	20311.943(-40)	19850.946(13)	
25		20338.218(-37)	19853.928(9)	20090.227(6)	20320.022(6)	19843.626(27)	
26		20347.047(3)	19846.929(10)	20091.157(67)	20327.900(73)	19836.375(-13)	
27		20355.740(109)	19840.047(-19)	20091.949(11)	20335.403(1)	19829.325(23)	
28		20364.011(6)	19833.369(6)	20092.748(-9)	20342.732(4)	19822.369(33)	
29		20372.131(-19)	19826.697(-106)		20349.798(5)	19815.468(-22)	
30		20380.023(-34)	19820.374(-10)	20094.236(-49)	20356.565(-16)	19808.745(-20)	
31		20387.709(0)	19814.089(-14)	20094.953(-24)	20363.096(12)	19802.206(47)	
32		20395.092(0)	19807.951(-3)		20369.219(-66)		
33		20402.166(-22)	19801.938(4)		20375.062(-110)		
34		20408.962(-21)	19796.004(-31)		20380.700(-34)		
35		20415.460(0)	19790.245(-8)		20385.972(12)		
36		20421.535(-64)	19784.603(21)				
37		20427.404(22)	19779.006(-6)				
38		20432.821(33)					
39		20437.799(4)					

		6 – 6			0 – 1		
N		R(N)	P(N)	Q(N)	R(N)	P(N)	Q(N)
6	*e*	20133.250(0)	20008.051(7)				
	f	20133.036(-9)	20007.719(11)				
7	*e*	20142.838(18)	19998.643(47)		18650.64(0)		
	f	20142.649(-11)	19998.311(-23)				
8	*e*	20152.332(-12)	19989.188(-30)		18664.81(-10)		18562.94(-5)
	f	20152.215(-6)	19988.987(-27)				

III. ANALYSIS

1. Description of the Observed Bands

The emission spectrum of the $\Delta v = 0$ sequence of BeD was observed in the 19 500–20 750 cm^{-1} region. An overview of the Fourier transform spectrum is displayed in Fig. 1. In addition to the BeD rotational lines, BeH lines belonging to the same sequence were observed in the spectrum. Some of these lines are clearly visible on the lower wavenumber side at 19 750 cm^{-1} (see Fig. 1). The presence of the BeH lines, due to H-containing impurities in the discharge, was very useful for the calibration of the wavenumber scale.

The $A^2\Pi$–$X^2\Sigma^+$ 0–0 to 6–6 bands of BeD were identified in our FT spectrum. The 3–3, 4–4, 5–5, and 6–6 bands were observed for the first time. All the observed bands have *P*, *Q*, and *R* branches, with a doublet fine-structure splitting resolved at low *N* values (up to $N = 10$) as appropriate for a Hund's case (b) $^2\Pi$–$^2\Sigma^+$ transition. An expanded portion of the spec-

TABLE 1—*Continued*

N		6 – 6			0 – 1		
		R(N)	P(N)	Q(N)	R(N)	P(N)	Q(N)
9	*e*	20161.814(1)	19979.899(-17)		18679.56(3)	18465.13(-8)	18566.44(-2)
	f	20161.700(-19)	19979.740(-17)				
10	*e*	20171.246(30)	19970.672(-20)		18694.34(-11)	18458.05(-4)	18570.29(-4)
	f	20171.126(-22)					
11		20180.569(27)	19961.487(-64)		18709.73(4)	18451.39(-5)	18574.24(-33)
12		20189.751(-31)	19952.500(2)		18725.35(12)	18445.22(-4)	18579.21(0)
13		20198.900(-26)	19943.496(-36)		18741.06(1)	18439.56(0)	18584.25(4)
14		20207.984(21)	19934.601(-60)		18757.15(0)	18434.33(0)	18589.54(-4)
15		20216.879(-1)	19925.873(-14)		18773.57(4)	18429.59(0)	18595.35(0)
16		20225.674(3)	19917.210(-4)		18790.18(1)	18425.34(1)	18601.46(0)
17		20234.343(22)	19908.661(17)		18806.93(-13)	18421.55(0)	18607.91(-5)
18		20242.837(17)	19900.188(10)		18824.20(0)	18418.32(5)	18614.77(-5)
19		20251.162(5)	19891.796(-22)		18841.41(-16)	18415.54(6)	18622.09(4)
20		20259.293(-26)	19883.486(-82)		18859.14(-3)	18413.03(-15)	18629.71(8)
21		20267.281(-14)	19875.467(40)		18877.05(6)	18411.25(-13)	18637.63(6)
22		20275.048(-27)	19867.500(104)		18894.97(-3)	18410.04(-5)	18645.76(-9)
23		20282.702(57)	19859.495(21)		18913.04(-18)	18409.16(-13)	18654.54(4)
24			19851.640(-23)		18950.22(0)	18409.16(15)	18663.49(1)
25			19843.937(-23)			18409.16(-5)	18672.73(-6)
26						18410.04(12)	18682.42(-2)
27						18411.25(12)	18692.41(-2)
28						18413.03(19)	18702.75(0)
29						18415.04(0)	
30						18417.79(5)	
31						18420.94(1)	

N	1 – 2			2 – 3		
	R(N)	P(N)	Q(N)	R(N)	P(N)	Q(N)
2						18662.09(-16)
3	18653.33(-37)					18663.49(25)
4	18666.24(-1)	18566.44(0)				18664.81(20)
5		18557.07(-18)	18612.43(-13)	18731.05(-23)	18612.43(2)	18666.24(-12)
6	18692.41(3)	18548.07(-42)	18614.77(-1)	18744.12(-1)	18603.64(-18)	18668.18(-28)
7	18705.85(-9)	18540.12(-5)	18617.20(-17)	18757.15(-15)	18595.35(-29)	18671.40(46)
8		18532.25(-3)	18620.26(-8)	18771.16(38)	18587.80(-9)	18673.69(-8)
9	18734.00(-3)		18623.63(-4)	18784.48(-6)		18676.97(1)
10	18748.51(-1)	18517.72(-11)	18627.35(-3)	18798.52(-7)	18573.60(-6)	18680.46(-2)
11		18511.28(0)	18631.43(-3)	18812.62(-30)	18567.17(-1)	18684.22(-15)
12	18778.30(-9)	18505.13(-4)	18635.86(-3)	18827.37(-14)	18561.12(-3)	18688.58(-3)
13	18793.71(-2)	18499.46(-6)	18640.66(-3)	18842.40(3)	18555.56(0)	18693.17(-2)
14	18809.20(-14)	18494.32(-2)	18645.87(0)	18857.54(6)	18550.42(1)	18698.02(-9)
15	18825.12(-10)	18489.60(-2)	18651.38(0)	18872.78(-3)	18545.68(-1)	
16	18841.41(8)	18485.34(-2)	18657.30(5)	18888.49(11)	18541.38(-6)	18708.95(-3)
17	18857.54(-14)	18481.56(-2)	18663.49(2)	18903.87(-29)	18537.66(1)	18714.96(3)
18	18874.24(-1)	18478.24(-2)	18670.05(1)	18920.32(16)	18534.34(3)	18721.24(4)
19	18891.04(0)	18475.37(-6)	18676.97(1)	18936.37(1)	18531.45(4)	18727.81(1)
20	18908.05(0)	18473.09(1)	18684.22(2)	18953.01(26)	18529.02(3)	18734.70(-1)
21	18925.01(-22)	18471.33(13)	18691.75(-3)		18527.03(0)	18741.92(-4)
22	18942.54(-8)	18469.89(9)	18699.65(-6)		18525.57(5)	18749.54(2)
23	18960.18(0)	18469.00(13)	18708.00(3)		18523.88(-60)	18757.15(-23)
24	18977.77(-14)	18468.46(2)	18716.55(0)		18523.88(-3)	18765.56(-1)
25		18468.46(-1)	18725.35(-9)		18523.88(7)	18774.08(3)
26		18469.00(0)	18734.70(4)		18523.88(-27)	18782.83(0)
27		18469.89(-11)	18744.12(-5)		18525.57(60)	18791.79(-10)
28		18471.33(-14)	18753.97(-2)		18526.28(2)	18801.37(11)
29		18473.52(7)	18764.19(5)		18528.00(1)	
30		18475.91(3)	18774.75(19)		18530.21(1)	
31		18478.85(5)	18785.30(2)		18532.85(0)	
32			18796.32(5)			

trum, displaying several *R* lines of the 0–0 to 6–6 bands, is presented in Fig. 2 (the presence of BeH lines can also be noticed in this figure as the unmarked lines).

While the $A^2\Pi$–$X^2\Sigma^+$ $\Delta v = 0$ sequence of BeH presents "extra" heads in all *P*, *Q*, and *R* branches at high *N* values (*1, 12*), no such features have been observed in the BeD spectrum for the assigned lines up to a maximum *N* value of 56 (in the 0–0 band). In common with the BeH spectrum is the presence of a "vibrational head" or "head-of-heads" for the *Q* branches of the $\Delta v = 0$ sequence. The origins of the $A^2\Pi$–$X^2\Sigma^+$ ($\Delta v = 0$) vibrational bands of BeD go initially to higher wavenumbers with $T_{00} = 20\,037.688\ \text{cm}^{-1}$, $T_{11} = 20\,054.105\ \text{cm}^{-1}$, $T_{22} = 20\,065.941\ \text{cm}^{-1}$, $T_{33} = 20\,073.011\ \text{cm}^{-1}$, and $T_{44} = 20\,075.202\ \text{cm}^{-1}$, and then they turn back to lower wavenumbers with $T_{55} = 20\,072.601\ \text{cm}^{-1}$ and $T_{66} = 20\,065.393\ \text{cm}^{-1}$. The vibrational head of BeD is formed at the 4–4 band, instead of the 3–3 band in the case of BeH. As one can see from the values given above, the origins of the 2–2

TABLE 1—*Continued*

	1 – 2			2 – 3		
N	R(N)	P(N)	Q(N)	R(N)	P(N)	Q(N)
30		18475.91(3)	18774.75(19)		18530.21(1)	
31		18478.85(5)	18785.30(2)		18532.85(0)	
32			18796.32(5)			

	3 – 4			4 – 5		
N	R(N)	P(N)	Q(N)	R(N)	P(N)	Q(N)
4	18767.51(16)					
5	18779.54(2)			18824.20(8)		
6	18791.79(-19)			18836.01(-21)		18764.19(-32)
7	18804.69(-7)	18647.17(-11)		18848.50(-11)		18766.70(-6)
8	18817.78(-5)	18639.38(-30)	18723.21(-12)	18860.81(-47)	18687.93(-3)	18769.31(-5)
9	18830.95(-22)	18632.23(-24)	18726.38(0)	18874.24(3)	18680.46(-46)	18772.21(-5)
10	18844.83(5)	18625.50(-19)	18729.74(0)	18887.11(-27)		18775.45(-5)
11	18858.62(-1)	18619.43(11)	18733.41(-5)	18900.58(-21)	18668.18(15)	18779.02(-3)
12	18872.78(1)	18613.38(1)	18737.47(-3)	18914.73(28)	18662.09(-9)	18782.83(-10)
13	18887.11(-1)	18607.91(7)	18741.92(4)	18928.05(-27)	18656.78(2)	18787.05(-6)
14		18602.70(-3)	18746.53(-3)	18942.54(12)	18651.38(-34)	18791.79(18)
15	18916.52(0)	18598.03(-2)	18751.60(0)	18956.50(-20)	18647.17(5)	18796.32(-9)
16		18593.78(-3)	18757.15(21)	18971.07(-13)	18642.90(-2)	18801.37(-15)
17	18946.82(4)	18589.98(-4)	18762.57(-3)		18639.38(21)	18806.93(-1)
18	18962.22(3)	18586.60(-6)	18768.53(-5)		18635.85(2)	18812.62(-3)
19	18977.77(-2)	18583.68(-6)	18774.75(-12)		18632.95(4)	18818.79(12)
20		18581.24(-3)	18781.47(0)		18630.38(-3)	18825.12(14)
21		18579.14(-11)	18788.36(-2)		18628.35(-1)	18831.57(0)
22			18795.61(1)		18626.74(0)	18838.41(-3)
23			18803.10(0)		18625.50(-4)	18845.61(0)
24			18810.89(-1)		18624.67(-13)	18853.13(6)
25			18818.79(-19)		18624.67(17)	18860.81(1)
26			18827.37(1)		18624.67(4)	18868.78(-1)
27			18836.01(0)		18625.50(30)	18877.05(-2)
28			18844.83(-10)		18626.28(5)	18885.82(20)
29			18854.08(-5)		18627.78(8)	18894.50(5)
30			18863.45(-14)		18629.71(8)	
31			18873.27(-5)		18632.23(21)	
32			18883.31(1)		18635.03(15)	
33					18638.35(13)	
34			18903.87(-13)		18642.15(12)	
35			18914.73(0)			
36			18925.67(-1)			
37			18937.00(11)			
38			18948.24(-7)			

	5 – 6				5 – 6		
N	R(N)	P(N)	Q(N)	N	R(N)	P(N)	Q(N)
4	18854.08(-11)			17		18685.67(-3)	18848.50(-2)
5	18865.91(26)		18805.76(-12)	18		18682.42(-2)	18854.08(5)
6	18877.05(-33)		18807.64(-10)	19		18679.56(-3)	18859.85(3)
7	18889.53(13)		18809.92(0)	20		18676.97(-21)	18865.91(2)
8	18901.59(-6)		18812.62(21)	21		18675.26(7)	18872.31(6)
9	18914.25(8)		18815.16(-3)	22		18673.69(5)	18878.83(-5)
10	18926.72(-19)		18818.79(47)	23		18672.73(22)	18885.82(1)
11	18939.87(-3)		18821.73(0)	24		18671.80(-2)	
12	18953.01(-10)	18708.00(-20)	18825.12(-32)	25		18671.40(-18)	
13		18702.75(-14)	18829.50(3)	26		18671.80(0)	
14	18980.00(-13)	18698.02(3)	18833.76(-2)	27		18672.73(28)	
15		18693.17(-31)	18838.41(0)	28		18673.69(14)	
16		18689.33(-5)	18843.19(-13)				

to 6–6 bands are separated only by a few wavenumbers so that extensive overlapping of lines occurs. In particular, the 5–5 Q branch is completely overlapped by the stronger 3–3 and 4–4 Q branches, while the 6–6 Q branch is completely obscured by the much stronger 2–2 Q branch. For these reasons we were not able to identify any 5–5 or 6–6 Q lines in the spectrum.

Strong rotational perturbations were observed in the $A^2\Pi$–$X^2\Sigma^+$ ($\Delta v = 0$) sequence of BeH (*1*) due to the interaction between the $A^2\Pi$ and the $C^2\Sigma^+$ states (*9*). In the case of BeD, the observed rotational levels of the $A^2\Pi$ state were not high enough in energy to reach the $C^2\Sigma^+$ levels and no perturbations were observed.

To derive the vibrational intervals, the analysis of a previously recorded arc emission spectrum (*9*) of the $A^2\Pi$–$X^2\Sigma^+$ ($\Delta v = -1$) sequence of BeD was carried out. The 0–1 to 5–6 bands were identified in the 18 400–19 000 cm^{-1} spectral region. Because of the positive $B' - B''$ difference which is greater than in the $\Delta v = 0$ sequence, the $\Delta v = -1$ bands form "classical" P heads. These heads are clearly visible for the 0–1, 1–2, and 2–3 bands, while for the 3–4, 4–5, and 5–6 bands

TABLE 2
Effective Constants (in cm^{-1}) for the $v = 0–6$ Vibrational Levels of the $X^2\Sigma^+$ Ground State of BeD

v	T_v	B_v	$D_v\times10^4$	$H_v\times10^8$	$L_v\times10^{12}$
0	0	5.624798(109)	3.11768(180)	1.6238(110)	-0.8746(219)
1	1488.7804(234)	5.4986379(989)	3.09752(173)	1.6170(114)	-0.9765(254)
2	2936.0845(273)	5.371270(129)	3.07908(272)	1.5850(215)	-1.0841(563)
3	4341.1713(338)	5.242847(215)	3.08004(569)	1.6631(583)	-1.655(204)
4	5703.1792(366)	5.111986(216)	3.08885(531)	1.6834(502)	-2.010(159)
5	7020.8525(557)	4.977028(444)	3.1002(148)	1.751(198)	-2.993(251)
6	8292.4575(578)	4.835962(290)	3.07073(881)	0.8755(799)	-

Note. All uncertainties are 1σ.

they become less prominent as the intensity decreases and heavy overlaps occur from the stronger Q and R branches of the lower v bands. It was possible to follow the P lines beyond the heads for all bands except the 3–4 band. The Q branches could also be followed up to relatively high N values, but the R branches were limited to lower N values because the available spectrum was cut at 19 000 cm^{-1}. Since the Q branch was not observed in the diagonal 5–5 band, the assignment of the 5–6 Q lines was very useful in determining the Λ-doubling parameters for the $A^2\Pi$ $v = 5$ level.

2. *Theoretical Model and Least-Squares Treatment*

We used the usual effective $\hat{\mathbf{N}}^2$ Hamiltonian for $^2\Sigma$ and $^2\Pi$ states (*13*) to reduce the experimental data to molecular constants. Explicit matrix elements for $^2\Sigma$ and $^2\Pi$ states are provided in Refs. (*14*) and (*15*). The $A^2\Pi$ and $X^2\Sigma^+$ electronic states of BeD both belong to the Hund's case (b) coupling case and this led to strong correlation between the spin–rotation parameters γ' and γ''. No satellite branches were detected so γ'' could not be directly determined. We have therefore chosen to fix the ground state γ constant to zero and to vary the corresponding γ constant in the upper state. The Λ-doubling constant p also could not be determined because of the nearly pure case (b) coupling in the $A^2\Pi$ state.

The experimental lines were fitted using a nonlinear, least-squares procedure with each datum weighted with the square of the reciprocal of the estimated uncertainty. The unblended FTS lines were assigned a weighting factor of 0.01 cm^{-1}, while the $\Delta v = -1$ data were weighted at 0.05 cm^{-1} for the strongest lines and 0.1 cm^{-1} for the weaker ones. However, the measurements of the blended lines were very imprecise in the arc emission spectrum and were heavily deweighted in the fits.

A first step in the least-squares treatment was to perform band-by-band fits of the $\Delta v = 0$ diagonal bands. In the ground

TABLE 3
Molecular Constants (in cm^{-1}) for the $v = 0–6$ Vibrational Levels of the $A^2\Pi$ State of BeD[a]

Constant	v=0	v=1	v=2	v=3	v=4	v=5	v=6
T_{v0}	20037.68838(216)	21542.8860(233)	23002.0259(273)	24414.1825(326)	25778.3817(352)	27093.4538(512)	28357.8505(578)
B_v	5.695744(108)	5.5607760(944)	5.423576(127)	5.284580(189)	5.142702(191)	4.995789(389)	4.843414(286)
$D_v\times10^4$	3.16701(179)	3.15879(159)	3.14859(263)	3.15891(483)	3.18246(453)	3.1835(122)	3.16793(889)
$H_v\times10^8$	1.5743(109)	1.5721(101)	1.5184(206)	1.5801(479)	1.6781(411)	1.496(156)	0.8199(879)
$L_v\times10^{12}$	-0.9078(217)	-1.0286(219)	-1.0953(536)	-1.583(162)	-2.208(125)	-2.354(679)	-
A_v	2.1592(133)	2.1930(277)	2.2378(500)	2.3390(738)	2.2901(999)	2.576(195)	2.5219(919)
$\gamma_v\times10^2$	-0.8015(277)	-0.7732(308)	-0.9242(529)	-1.0518(670)	-1.1186(743)	-1.398(135)	-1.299(920)
$\gamma_{Dv}\times10^5$	0.8069(479)	0.7536(514)	1.138(103)	1.443(140)	1.587(150)	2.279(304)	1.745(206)
$\gamma_{Hv}\times10^9$	-2.218(196)	-2.043(203)	-3.983(482)	-5.701(737)	-6.244(747)	-1.041(176)	-
$q_v\times10^3$	4.2192(140)	4.0579(133)	3.88937(858)	3.7632(185)	3.5963(361)	3.394(338)	3.355[b]
$q_{Dv}\times10^7$	-9.172(186)	-8.663(214)	-8.5847(724)	-9.208(226)	-10.892(640)	-9.62(674)	-10.261[b]
$q_{Hv}\times10^{11}$	5.399(638)	2.495(802)	-	-	-	-	-

Note. All uncertainties are 1σ.

[a] The fine structure parameters A_v, γ_v, γ_{Dv}, γ_{Hv} were fixed in the global fit at values determined from the $\Delta v = 0$ separate fits. The uncertainties reported here are also taken from the $\Delta v = 0$ fits.

[b] Fixed at linearly extrapolated values from the $v = 0–3$ data.

TABLE 4
Dunham Constants (in cm^{-1}) for the $X^2\Sigma^+$ Ground State of BeD

	$m = 0$	$m = 1$	$m = 2$	$m = 3$	$m = 4$
$Y_{0,m}$		5.68821540(5045)	$-3.1406219(7370)\times10^{-4}$	$1.688217(4643)\times10^{-8}$	$-9.25625(9354)\times10^{-13}$
$Y_{1,m}$	1529.82676(5851)	-0.1267355(1058)	$4.8910(1018)\times10^{-6}$	$-1.36175(5710)\times10^{-9}$	$9.903(1094)\times10^{-14}$
$Y_{2,m}$	-20.28494(5739)	$1.0733(7675)\times10^{-4}$	$-1.26569(4103)\times10^{-6}$	$5.5366(1531)\times10^{-10}$	$-6.2324(2813)\times10^{-14}$
$Y_{3,m}$	-0.17547(2554)	$8.987(2571)\times10^{-5}$	$8.1087(9522)\times10^{-8}$	$-6.70232(9450)10^{-11}$	
$Y_{4,m}$	$3.6008(5851)\times10^{-2}$	$-6.9903(4184)\times10^{-5}$	$1.4062(1172)\times10^{-8}$		
$Y_{5,m}$	$-6.8078(7071)\times10^{-3}$	$8.0539(3217)\times10^{-6}$	$-1.76381(5016)\times10^{-9}$		
$Y_{6,m}$	$4.7642(4235)\times10^{-4}$	$-3.46519(9351)\times10^{-7}$	$-2.60859(6180)\times10^{-8}$		
$Y_{7,m}$	$-1.54592(9887)\times10^{-5}$				

Note. All uncertainties are 1σ.

$X^2\Sigma^+$ electronic state it was possible to determine the rotational constants B, D, H, and L except for $v = 6$ where limited data gave only B, D, and H. A similar set of rotational parameters was required for the $A^2\Pi$ state along with the Λ-doubling series q, q_D, and q_H as well as for the spin–orbit coupling constant A and the spin–rotation constants γ, γ_D, and γ_H (*16*). As no Q lines were observed for the 5–5 and 6–6 bands, the q and q_D parameters for the $A^2\Pi$ $v = 5$ and $v = 6$ levels were fixed in the 5–5 and 6–6 fits at values obtained by linearly extrapolating the $v = 0$–3 values.

The second step of the analysis was to perform a global fit of all the observed bands (0–0 to 6–6 in the $\Delta v = 0$ sequence and 0–1 to 5–6 in the $\Delta v = -1$ sequence). The values derived from the band-by-band fits of the $\Delta v = 0$ diagonal bands were used as a starting point for the constants in the global fit. Because no fine-structure splitting could be observed on the lower resolution $\Delta v = -1$ spectrum, we decided to fix the fine-structure constants A_v, γ_v, γ_{Dv}, and γ_{Hv} in the global fit at values determined from the $\Delta v = 0$ separate fits. However, the $\Delta v = -1$ bands gave useful information for determining the Λ-doubling parameters q and q_D in the $A^2\Pi$ $v = 5$ level. Through the observation of the 5–6 Q branch, these parameters varied freely in the global fit, in contrast to the 5–5 fit where they were kept fixed. No experimental Λ-doubling information was available for the $A^2\Pi$ $v = 6$ level, so the q and q_D constants in the global fit had to be kept fixed at extrapolated values.

The assigned lines of the $A^2\Pi$–$X^2\Sigma^+$ $\Delta v = 0$ and $\Delta v = -1$ sequences of BeD are listed in Table 1.The "observed − calculated" differences returned by the global fit are presented in parentheses, in the units of the last quoted digit. Note that the lines with unresolved fine structure were included twice in the fit, corresponding to the two parities (e/f) of a given lower rotational level N. For these lines, we have arbitrarily chosen to report only the "observed − calculated" differences for the e parity in the lower state. The molecular constants derived from the global fit (except for the A_v, γ_v, γ_{Dv}, and γ_{Hv} constants, which are derived from the band-by-band $\Delta v = 0$ fits; see above) are listed in Tables 2 and 3, for the $X^2\Sigma^+$ and the $A^2\Pi$ states, respectively.

III. DISCUSSION

Since we have arbitrarily set the spin–rotation constant γ'' to zero in the ground state, the excited state constant γ' is, in fact, the difference $\gamma' - \gamma''$. In this respect, the $A^2\Pi$–$X^2\Sigma^+$ transition is like a $^2\Sigma$–$^2\Sigma$ transition. It is possible to estimate a value of $\gamma'' = 1(1) \times 10^{-3}$ cm^{-1} for the ground state using Curl's relationship (*17, 18*), $\gamma = 2B\Delta g$, and the small anisotropy of the g tensor of matrix-isolated BeD (*19*). A crude estimate based on a pure precession relationship (*20*) between the ground state and the $A^2\Pi$ state gives a similar value of $\gamma'' = 2 \times 10^{-3}$ cm^{-1}.

1. Vibrational Analysis

The previous absorption study of the $A^2\Pi$–$X^2\Sigma^+$ system of BeD by Horne and Colin (*5*) provided spectroscopic information on the $v = 0$, 1, and 2 vibrational levels of the $X^2\Sigma^+$

TABLE 5
Main Equilibrium Constants (in cm^{-1}) of the $A^2\Pi$ State of BeD[a,b]

$T_e = 20027.8504(219)$	
$\omega_e = 1550.2599(143)$	$B_e = 5.762283(390)$
$\omega_e x_e = 22.2083(129)$	$\alpha_e = 0.132261(875)$
$\omega_e y_e = -0.21900(481)$	$\gamma_{1e} = -1.709(567)\times10^{-3}$
$\omega_e z_{1e} = 1.5277(785)\times10^{-2}$	$\gamma_{2e} = 2.53(133)\times10^{-4}$
$\omega_e z_{2e} = -1.3616(464)\times10^{-3}$	$\gamma_{3e} = -3.16(102)\times10^{-5}$

Note. All uncertainties are 1σ.

[a] $G_v = \omega_e(v + 1/2) - \omega_e x_e(v + 1/2)^2 + \omega_e y_e(v + 1/2)^3 + \omega_e z_{1e}(v + 1/2)^4 + \omega_e z_{2e}(v + 1/2)^5$.

[b] $B_v = B_e - \alpha_e(v + 1/2) + \gamma_{1e}(v + 1/2)^2 + \gamma_{2e}(v + 1/2)^3 + \gamma_{3e}(v + 1/2)^4$.

TABLE 6
Effective Constants (in cm^{-1}) for the $A^2\Pi$–$X^2\Sigma^+$ (0–0, 1–1, 2–2, and 3–3) Transition of BeT[a]

	$A^2\Pi - X^2\Sigma^+$			
Constant	0 – 0	1 – 1	2 – 2	3 – 3
$T_{vv'}$	20039.7739(162)	20054.1972(165)	20065.4360(223)	20072.9255(245)
B'_v	4.153553(493)	4.079661(560)	3.987562(909)	3.88892(131)
B''_v	4.103976(497)	4.035324(569)	3.949513(945)	3.85508(126)
$D'_v \times 10^4$	1.64210(610)	1.93122(737)	1.7287(221)	1.0889(435)
$D''_v \times 10^4$	1.64505(619)	1.95921(695)	1.7315(234)	1.0869(405)
$H'_v \times 10^8$	0.3411(235)	1.2244(326)	4.52(110)	-7.022(449)
$H''_v \times 10^8$	0.5625(232)	1.6094(249)	4.52(118)	-5.869(401)
$\gamma'_v \times 10^2$	-0.8705(920)	-0.964(101)	-1.062(150)	-1.329(211)
$\gamma'_{Dv} \times 10^6$	5.611(825)	6.771(977)	8.76(186)	16.75(473)
$q'_v \times 10^3$	3.063(143)	3.214(161)	3.961(215)	2.714(196)
$q'_{Dv} \times 10^6$	-3.982(369)	-4.060(515)	-7.199(654)	-2.187(466)
$q'_{Hv} \times 10^9$	3.362(214)	3.179(398)	4.969(446)	-

Note. All uncertainties are 1σ.
[a] The A parameter in the $A^2\Pi$ ($v = 0$–3) state was fixed at 2.15 cm^{-1} (see text).

ground state. In the present work, we extend the knowledge of the vibrational levels of the ground state to the $v = 3$–6 levels. There is also additional information available for the $X^2\Sigma^+$ $v = 8$–12 vibrational levels from the study of the $C^2\Sigma^+$–$X^2\Sigma^+$ transition (0–8 to 0–12 bands) of BeD (*9*). Unfortunately, we could not directly link the $v = 0$–6 levels observed in this work with the $v = 8$–12 levels, as we did recently for the BeH ground state (*1*). However, the experimental data for the $v = 8$–12 levels of the ground state can be used via the combination differences in a fit to Dunham Y's (*10*). Because the $C^2\Sigma^+$ $v = 0$ level is massively perturbed, only the ground state combination differences were introduced into our fit. In addition to the usual rotational differences, all the possible differences between P lines and R lines with the same N'', N', and v' but different v'' were added to the fit in order to obtain the $X^2\Sigma^+$ vibrational intervals. In this way, the vibrational energy levels for $v = 0$–6 and 8–12 of the ground state were fitted together. The ground state rovibrational energies were represented by the conventional double Dunham expansion (*10*),

$$E_X(v'', N'') = \sum_{l,m} Y''_{l,m}(v'' + \tfrac{1}{2})^l[N''(N'' + 1)]^m, \qquad [1]$$

and the upper $A^2\Pi$ levels were represented by the $^2\Pi$ matrix discussed above. The $A^2\Pi$ constants were kept fixed at the values listed in Table 3. The values of the $Y''_{l,m}$ parameters obtained for the $X^2\Sigma^+$ ground state of BeD are listed in Table 4. However, it should be noted that the normalized standard deviation of 1.6 of this fit was somewhat higher than the value of about 1 obtained in the $v = 0$–6 fit described above.

The Dunham constants of Table 4 are a relatively poor representation of the energy levels of BeD. The traditional constants form a badly convergent series with strong correlation between the parameters. It is, therefore, necessary to carry many extra significant figures in Table 4 and many of the terms (even ω_e) in the expansion have lost much of their physical meaning. Nevertheless, the Y's of Table 4 do reproduce the experimental data in an empirical manner. In future work, we plan to explore the fitting of the BeH and BeD data using alternate energy level expressions (*21*) as well as the direct fitting to a potential energy curve that includes Born–Oppenheimer breakdown terms (*22*).

The $A^2\Pi$ excited state vibrational and rotational constants from Table 3 were fitted with the traditional expressions to obtain the equilibrium constants listed in Table 5. The equilibrium bond length for the $A^2\Pi$ state was calculated to be 1.33309(4) Å compared to 1.341742(5) Å for the ground state, calculated from Y_{01} (Table 4).

2. *BeT Revisited*

The $A^2\Pi$–$X^2\Sigma^+$ 0–0, 1–1, 2–2, and 3–3 bands of BeT were recorded in emission by De Greef and Colin (*2*) using a Be hollow cathode discharge lamp and a 2-m Czerny–Turner spectrograph. They calibrated the wavelength scale using BeH lines present in the spectrum as an impurity and the absolute accuracy of the line positions was estimated to be ± 0.07 cm^{-1}.

We therefore decided to use the opportunity offered by our FTS study of the $A^2\Pi$–$X^2\Sigma^+$ system of BeH and BeD to recalibrate the $A^2\Pi$–$X^2\Sigma^+$ ($\Delta v = 0$) spectrum of BeT. Another reason for our reanalysis was to use the matrix-based fitting model described in the previous section, ensuring a consistent treatment of the data for the three isotopomers. The BeT line positions reported by De Greef and Colin (*2*) were adjusted by adding 0.02 cm^{-1}, on the basis of the new FTS measurements of BeH (*1*). The recalibrated rotational lines of the $A^2\Pi$–$X^2\Sigma^+$ 0–0 to 3–3 diagonal bands of BeT were fitted band-by-band using the theoretical model and the least-squares treatment described above for BeD. The effective parameters derived from the fits are listed in Table 6. Note that the A constant was fixed for all the studied levels ($v = 0$–3) of the upper $A^2\Pi$ state at 2.15 cm^{-1}, which is a typical value for BeH and BeD.

V. CONCLUSION

We have measured the 0–0 to 6–6 bands of the $A^2\Pi$–$X^2\Sigma^+$ transition of BeD with a Fourier transform spectrometer. The $A^2\Pi$–$X^2\Sigma^+$ 0–1 to 5–6 bands were identified in the $\Delta v = -1$ sequence in a previously recorded arc emission spectrum, which allowed us to link together all of the new FTS data. A global fit of the $\Delta v = 0$ and $\Delta v = -1$ bands was performed and molecular constants derived for the $X^2\Sigma^+$ ($v = 0$–6) and $A^2\Pi$ ($v = 0$–6) levels of BeD. The data for the $X^2\Sigma^+$ ($v = 8$–12) levels, available from the $C^2\Sigma^+$–$X^2\Sigma^+$ study (*9*), were used via the combination differences in a Dunham fit, including the $v = 0$–6 and 8–12 vibrational levels of the $X^2\Sigma^+$ ground state. A vibrational analysis was also carried out for the $A^2\Pi$ excited state using the traditional expressions (Table 5) to obtain equilibrium constants. The previously published $A^2\Pi$–$X^2\Sigma^+$ 0–0 to 3–3 bands of BeT (*2*) were recalibrated using the new FTS data and reanalyzed using the same theoretical model as in the study of BeH (*1*) and BeD.

ACKNOWLEDGMENTS

This work was supported by the Fonds National de la Recherche Scientifique (Belgium) and the Natural Sciences and Engineering Research Council of Canada. C.F. thanks the Université des Sciences et Technologies de Lille (France) for a BQR grant.

REFERENCES

1. C. Focsa, S. Firth, P. Bernath, and R. Colin, *J. Chem. Phys.* (in press).
2. D. De Greef and R. Colin, *J. Mol. Spectrosc.* **53,** 455–465 (1974).
3. J. M. L. Martin, *Chem. Phys. Lett.* **283,** 283–293 (1998).
4. P. G. Koontz, *Phys. Rev.* **48,** 707–713 (1935).
5. R. Horne and R. Colin, *Bull. Soc. Chim. Belg.* **81,** 93–107 (1972).
6. R. Colin and D. De Greef, *Can. J. Phys.* **53,** 2142–2169 (1975).
7. C. Clerbaux and R. Colin, *Mol. Phys.* **72,** 471–486 (1991).
8. G. Duxbury, M. F. Stamp, and H. P. Summers, *Plasma Phys. Contr. Fus.* **40,** 361 (1998).
9. R. Colin, C. Drèze, and M. Steinhauer, *Can. J. Phys.* **61,** 641–655 (1983).
10. J. L. Dunham, *Phys. Rev.* **41,** 721–731 (1932).
11. B. A. Palmer and R. Engleman, Jr., "Atlas of the Thorium Spectrum," Los Alamos National Laboratory, 1983.
12. G. Herzberg, "Spectra of Diatomic Molecules," 2nd ed., Van Nostrand–Reinhold, New York, 1950.
13. J. M. Brown, E. A. Colbourne, J. K. G. Watson, and F. D. Wayne, *J. Mol. Spectrosc.* **74,** 294–318 (1979).
14. M. Douay, S. A. Rogers, and P. F. Bernath, *Mol. Phys.* **64,** 425–436 (1988).
15. C. Amiot, J.-P. Maillard, and J. Chauville, *J. Mol. Spectrosc.* **87,** 196–218 (1981).
16. J. M. Brown and J. K. G. Watson, *J. Mol. Spectrosc.* **65,** 65–74 (1977).
17. R. F. Curl, Jr., *J. Chem. Phys.* **37,** 779–784 (1962).
18. W. Weltner, Jr., "Magnetic Atoms and Molecules," Dover, New York, 1990.
19. L. B. Knight, Jr., J. M. Brom, Jr., and W. Weltner, Jr., *J. Chem. Phys.* **56,** 1152–1155 (1972).
20. J. H. Van Vleck, *Phys. Rev.* **33,** 467–506 (1929).
21. D. T. Appadoo, R. J. LeRoy, P. F. Bernath, S. Gerstenkorn, P. Luc, J. Vergès, J. Sinzelle, J. Chevillard, and Y. D'Aignaux, *J. Chem. Phys.* **104,** 903–913 (1996).
22. M. Dulick, K.-Q. Zhang, B. Guo, and P. F. Bernath, *J. Mol. Spectrosc.* **188,** 14–26 (1998).